

Supporting Information

Directed Self-Assembly of Rhombic Carbon Nanotube Nanomesh Films for Transparent and Stretchable Electrodes

Sehee Ahn,^{‡a} Ayoung Choe,^{‡a} Jonghwa Park,^a Heesuk Kim,^b Jeong Gon Son,^b Sang-Soo Lee,^{b,c} Min Park,^d and Hyunhyub Ko^{*a}

^a School of Energy and Chemical Engineering, Ulsan National Institute Science and Technology (UNIST), Ulsan Metropolitan City, 689-798, Republic of Korea. *E-mail: hyunhko@unist.ac.kr

^b Photo-Electronic Hybrids Research Center, Korea Institute of Science and Technology, Seoul 136-791, Republic of Korea.

^c KU-KIST Graduate School of Converging Science and Technology, Korea University, Seoul 136-701, Republic of Korea.

^d Soft Innovative Materials Research Center, Korea Institute of Science and Technology, Jeonbuk, 565-905, Republic of Korea.

‡ These authors contributed equally to this work.

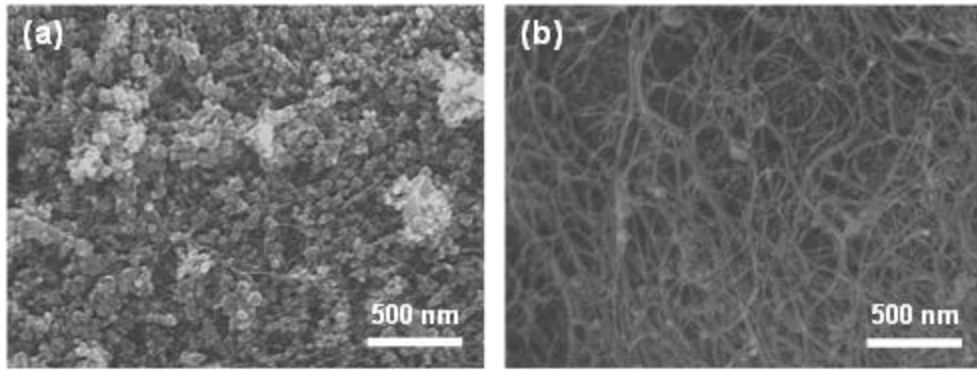


Fig. S1. SEM images of (a) as-produced SWNTs and (b) purified SWNTs. (c) Procedures of SWNT purification.

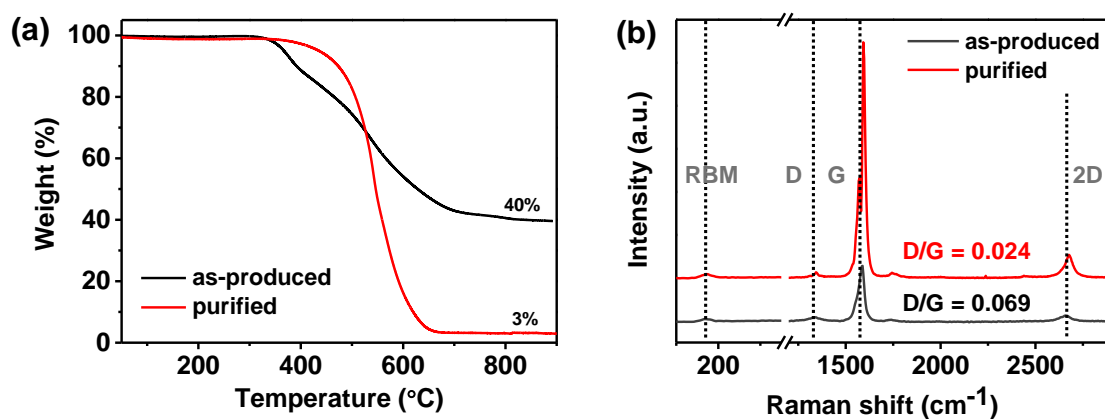


Fig. S2. (a) Thermo gravimetric analysis of as-produced, annealed, purified, and centrifuged SWNTs. The purity of SWNTs improved from 60% to 97% after purification. (b) Raman spectra of as-produced, annealed and purified SWNTs. Both of as-produced and purified SWNTs show Raman RBM, D, G, and 2D modes. The D/G ratios decreased from 0.069 to 0.024 after purification, indicating the removal of disordered carbons.

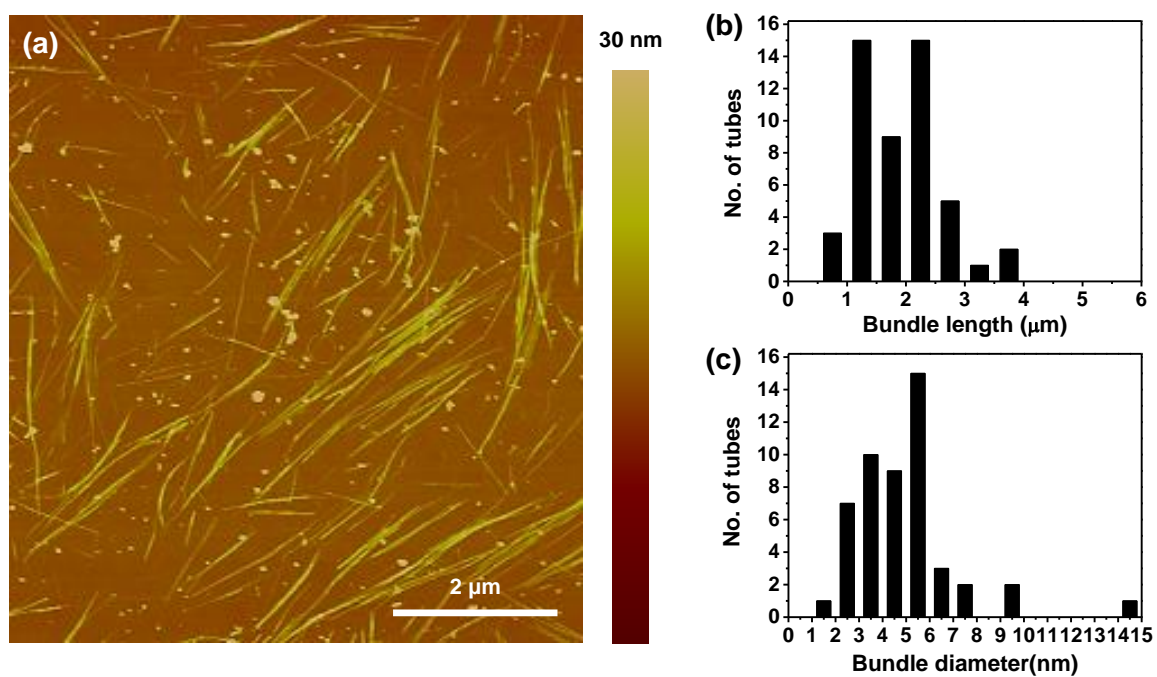


Fig. S3. (a) AFM image of the SWNT on silicon wafer. Statistical analyses of (c) length and (d) height distributions of SWNTs. SWNTs show an average length of 1.9 μm and diameter of 4.9 nm.

Line-patterned PDMS mold

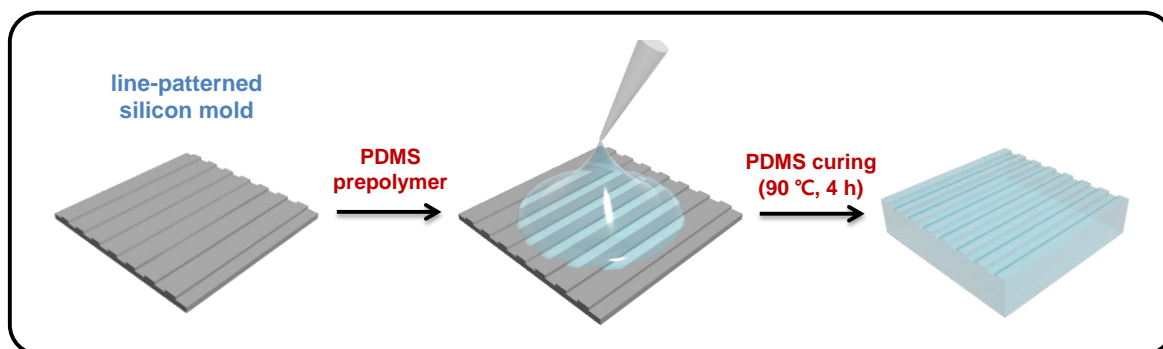


Fig. S4. Schematic illustration of the fabrication of a line-patterned PDMS mold.

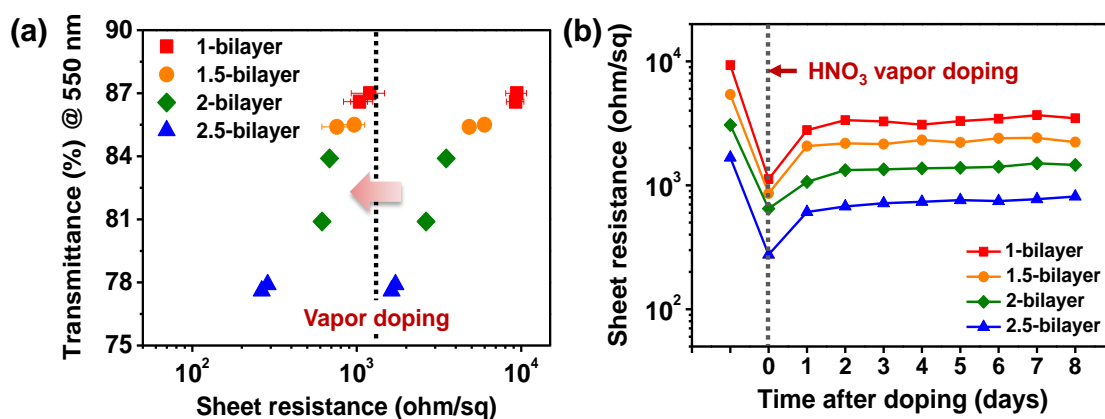


Fig. S5. (a) Transmittance and sheet resistance of SWNT films before and after nitric acid vapor doping. SWNT films after the nitric acid vapor doping showed about 6 times lower sheet resistance than those without doping at similar transmittance. (b) The change of sheet resistance of SWNT films as a function of time after nitric acid vapor doping.

The nitric acid vapor exposure onto SWNT films is responsible for the oxidation of SWNTs, which induces charge transfer from SWNT to adsorbates and thus provides p-type doping of SWNTs. Here, both the simple adsorbates of HNO₃ on the nanotube surface and the intercalated ones with the nanotube bundles can contribute to the charge transfer doping.^{11,12} In this doping method, the chemical doping is not completely stable since the small molecules adsorbed on the CNTs can desorb with time. As can be seen in Figure S5b, the sheet resistance of SWNT films gradually increases with time after acid vapor doping. To increase the doping stability, recently, new strategies such as MoOx doping have been suggested.¹³

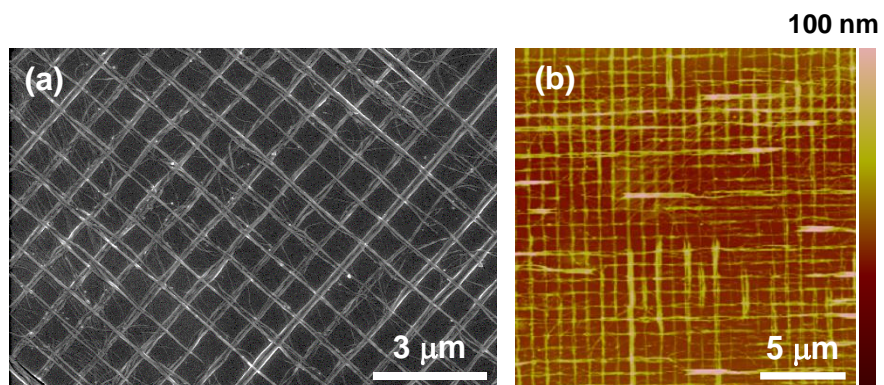


Fig. S6. Representative (a) SEM and (b) AFM images of LbL assembled SWNT nanomesh films showing the long range ordered structures.

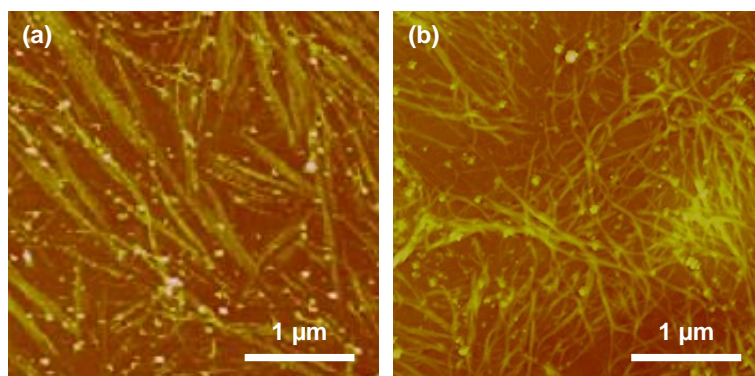


Fig. S7. AFM images of non-regular SWNT films. (a) Locally aligned SWNT films prepared by spin-coating. (b) Randomly deposited SWNT films prepared by vacuum filtration.

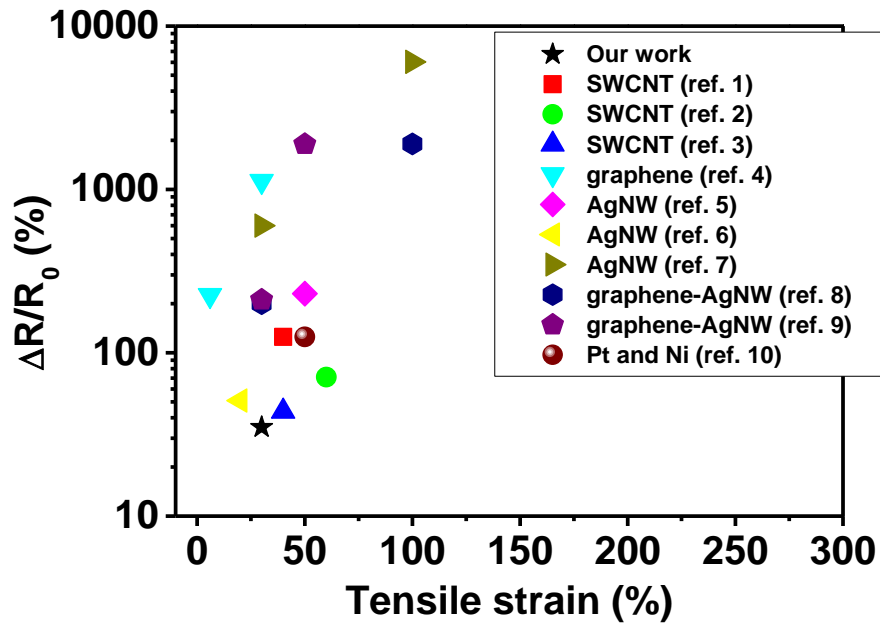


Fig. S8. Comparison of the stretchable performance of the nanomesh-structured SWNT films with various stretchable and transparent conductive films. The two points of reference 4 mean graphene films transferred on unstrained or pre-strained PDMS. The estimated changes of resistance at 30 % tensile strain were added to reference 7-9 to compare the stretchability with our nanomesh-structured SWNT film at same tensile strain.

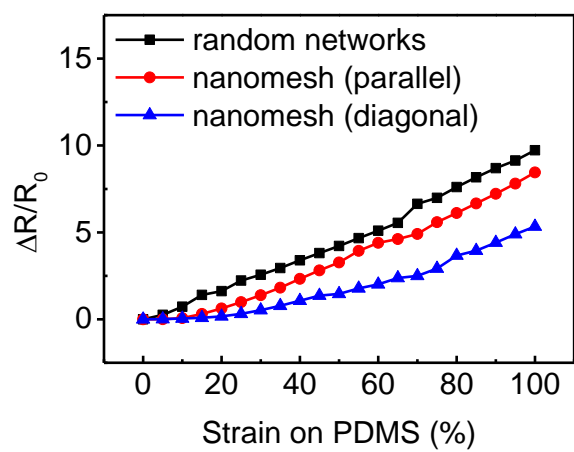


Fig. S9. Variations in resistance of SWNT networks as a function of tensile strain up to 100 %.

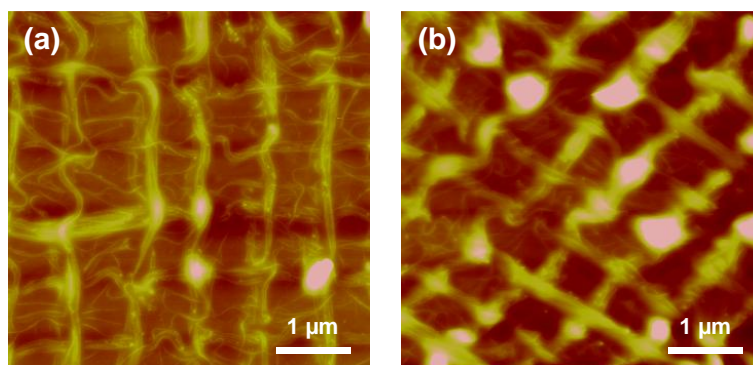


Fig. S10. AFM images of SWNT nanomesh films on PDMS after 10 times of repetitive stretching and relaxation processes (30 % strain) in the (a) parallel and (b) diagonal directions.

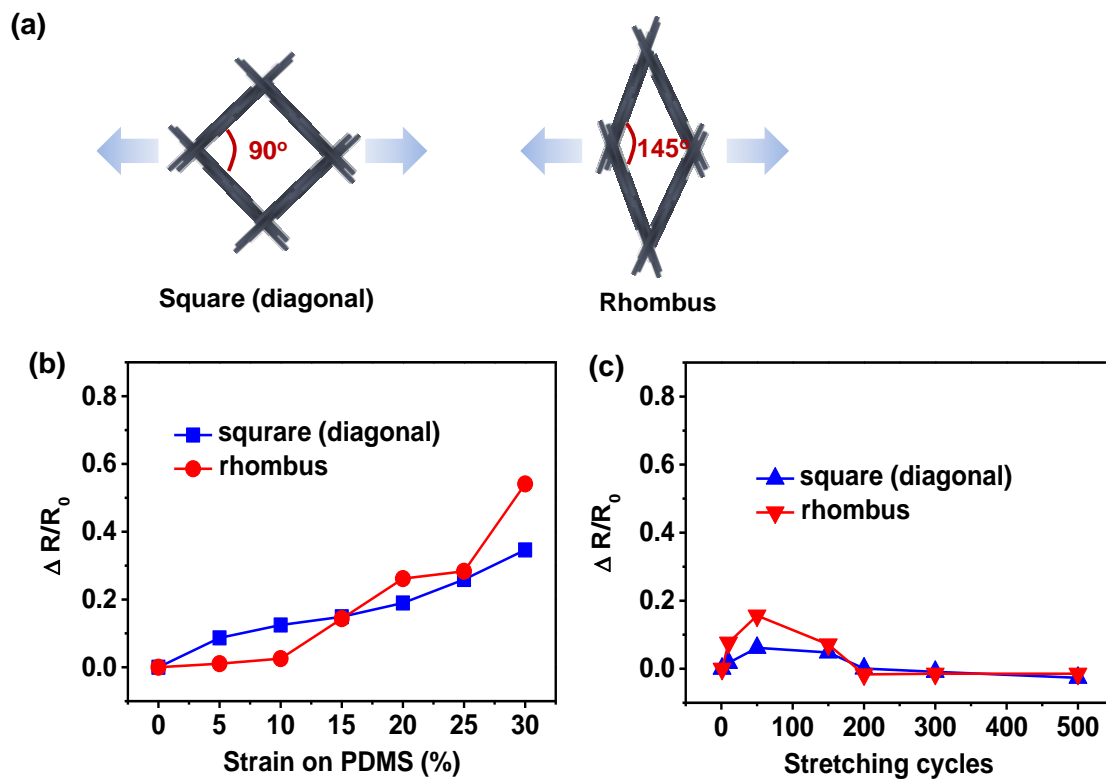


Fig. S11. Effects of the interior angles of rhombic nanomesh films on the stretchability. (a) Schematic of rhombic nanomesh films with different interior angles (90, 145 degrees). (b) Relative change in resistance as a function of tensile strain. (c) Durability of rhombic nanomesh films as a function of stretching cycle (30 % strain).

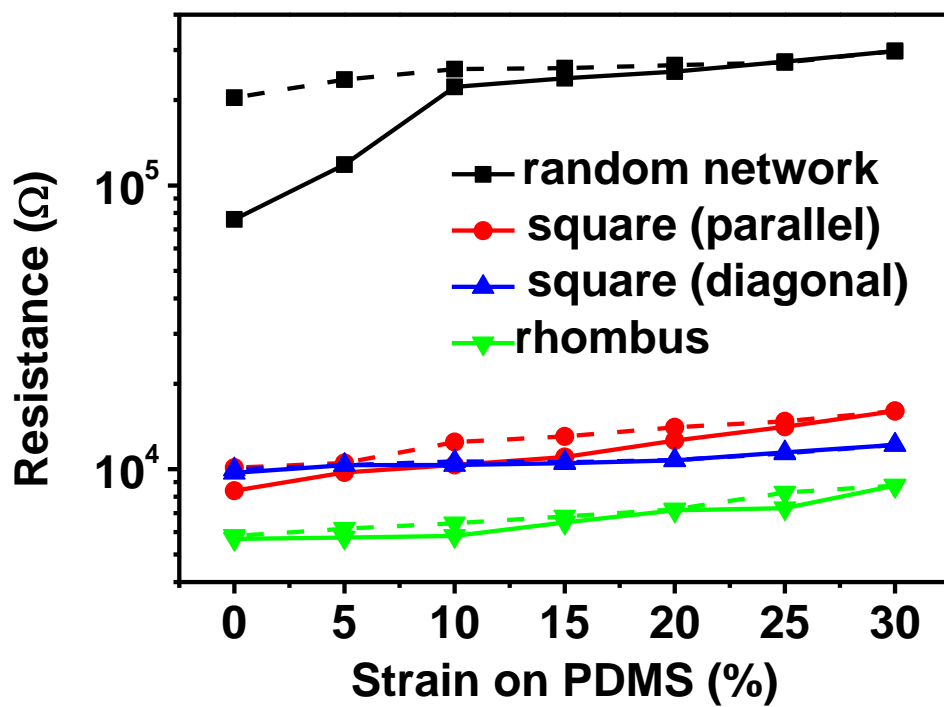


Fig. S12. Resistance change of SWNT films as a function of tensile strain for random, square nanomesh (parallel, diagonal), and rhombus nanomesh structures during stretching and releasing processes.

References

- 1 D. J. Lipomi, M. Vosgueritchian, B. C. Tee, S. L. Hellstrom, J. A. Lee, C. H. Fox, Z. Bao, *Nat. Nanotechnol.* 2011, **6**, 788-792.
- 2 L. Cai, J. Li, P. Luan, H. Dong, D. Zhao, Q. Zhang, X. Zhang, M. Tu, Q. Zeng, W. Zhou, *Adv. Funct. Mater.* 2012, **22**, 5238-5244.
- 3 C. Feng, K. Liu, J. S. Wu, L. Liu, J. S. Cheng, Y. Zhang, Y. Sun, Q. Li, S. Fan, K. Jiang, *Adv. Funct. Mater.* 2010, **20**, 885-891.
- 4 K. S. Kim, Y. Zhao, H. Jang, S. Y. Lee, J. M. Kim, K. S. Kim, J.-H. Ahn, P. Kim, J.-Y. Choi, B. H. Hong, *Nature* 2009, **457**, 706-710.
- 5 W. Hu, X. Niu, L. Li, S. Yun, Z. Yu, Q. Pei, *Nanotechnology* 2012, **23**, 344002.
- 6 T. Akter, W. S. Kim, *ACS Appl. Mater. Interfaces* 2012, **4**, 1855-1859.
- 7 J. Liang, L. Li, X. Niu, Z. Yu, Q. Pei, *Nat. Photonics* 2013, **7**, 817-824.
- 8 J. Liang, L. Li, K. Tong, Z. Ren, W. Hu, X. Niu, Y. Chen, Q. Pei, *ACS nano* 2014, **8**, 1590-1600.
- 9 H. Lee, K. Lee, J. T. Park, W. C. Kim, H. Lee, *Adv. Funct. Mater.* 2014, **24**, 3276-3283.
- 10 H. Wu, D. Kong, Z. Ruan, P.-C. Hsu, S. Wang, Z. Yu, T. J. Carney, L. Hu, S. Fan, Y. Cui, *Nat. Nanotechnol.* 2013, **8**, 421-425.
- 11 H. Gao, R. Izquierdo, and V.-V. Truong, *Chem. Phys. Lett.* 2012, **546**, 109-114.
- 12 R. Jackson, B. Domercq, R. Jain, B. Kippelen, and S. Graham, *Adv. Funct. Mater.* 2008, **18**, 2548-2554.
- 13 S. L. Hellstrom, M. Vosgueritchian, R. M. Stoltenberg, I. Irfan, M. Hammock, Y. B. Wang, C. C. Jia, X. F. Guo, Y. L. Gao, Z. N. Bao, *Nano Lett.* 2012, **12**, 3574-3580.